AIP Journal of Applied Physics

Enhanced optical property in quaternary GaInAsSb/AlGaAsSb quantum wells

Chien-Hung Lin and Chien-Ping Lee

Citation: Journal of Applied Physics **116**, 153504 (2014); doi: 10.1063/1.4898389
View online: http://dx.doi.org/10.1063/1.4898389
View Table of Contents: http://scitation.aip.org/content/aip/journal/jap/116/15?ver=pdfcov
Published by the AIP Publishing

Articles you may be interested in
Carrier localization and in-situ annealing effect on quaternary Ga1−xInxAsySb1−y/GaAs quantum wells grown by Sb pre-deposition
Appl. Phys. Lett. **102**, 113101 (2013); 10.1063/1.4795866

Much improved flat interfaces of In Ga As ∕ Al As Sb quantum well structures grown on (411) A InP substrates by molecular-beam epitaxya)
J. Vac. Sci. Technol. B **23**, 1158 (2005); 10.1116/1.1914818

Optically probed wetting layer in InAs/InGaAlAs/InP quantum-dash structures
Appl. Phys. Lett. **86**, 101904 (2005); 10.1063/1.1881782

Photoluminescence and photoreflectance study of InGaAs/AlAsSb quantum wells grown by molecular-beam epitaxy
J. Appl. Phys. **95**, 1050 (2004); 10.1063/1.1637936

Optical properties of InGaAs/AlAsSb type I single quantum wells lattice matched to InP
J. Vac. Sci. Technol. B **19**, 1747 (2001); 10.1116/1.1394727

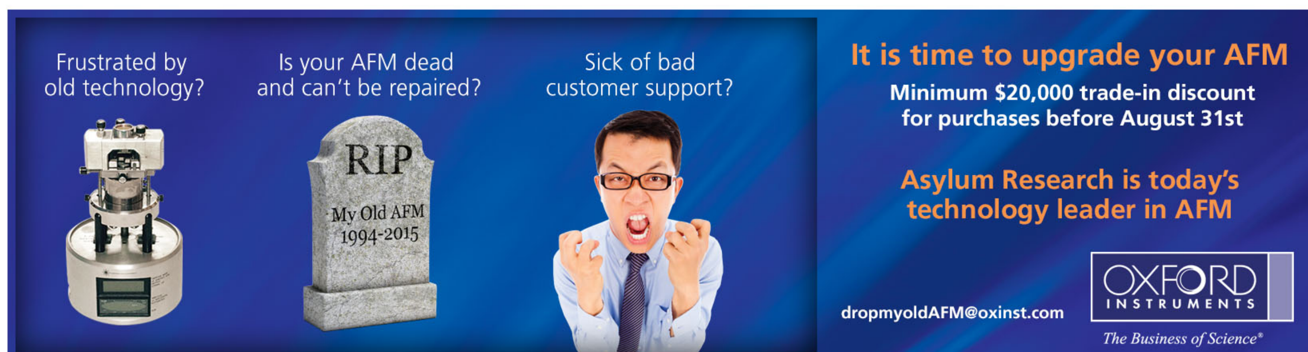

[This article is copyrighted as indicated in the article. Reuse of AIP content is subject to the terms at: http://scitation.aip.org/termsconditions. Downloaded to] IP: 140.113.38.11 On: Tue, 21 Jul 2015 10:10:05

JOURNAL OF APPLIED PHYSICS 116, 153504 (2014)

Enhanced optical property in quaternary GaInAsSb/AlGaAsSb quantum wells

Chien-Hung Lin[a] and Chien-Ping Lee
Department of Electronics Engineering, National Chiao Tung University, 1001 University Road, Hsinchu 30010, Taiwan

(Received 2 September 2014; accepted 6 October 2014; published online 16 October 2014)

High quality GaInAsSb/AlGaAsSb quantum wells (QWs) have been grown by molecular beam epitaxy using proper interface treatments. By controlling the group-V elements at interfaces, we obtained excellent optical quality QWs, which were free from undesired localized trap states, which may otherwise severely affect the exciton recombination. Strong and highly efficient exciton emissions up to room temperature with a wavelength of 2.2 μm were observed. A comprehensive investigation on the QW quality was carried out using temperature dependent and power dependent photoluminescence (PL) measurements. The PL emission intensity remains nearly constant at low temperatures and is free from the PL quenching from the defect induced localized states. The temperature dependent emission energy had a bulk-like behavior, indicating high quality well/barrier interfaces. Because of the uniformity of the QWs and smooth interfaces, the low temperature limit of inhomogeneous line width broadening is as small as 5 meV. © *2014 AIP Publishing LLC*.
[http://dx.doi.org/10.1063/1.4898389]

I. INTRODUCTION

Mid-infrared optoelectronic devices are of great interests due to their extensive applications in environmental monitoring, atmospheric gases sensing, medical diagnostics, and free space communications. Sb-based materials are commonly used in the mid-infrared light sources. To date, MBE grown GaInAsSb/AlGaAsSb quantum well (QW) systems, in particular, have demonstrated excellent lasing performances in the 2–3 μm range.[1–3] With the use of quinternary AlGaInAsSb barrier materials, the emission wavelength can even be extended to above 3 μm.[4,5] Obviously, good material quality leads to good optical properties. But in such complex structures with so many constituent elements, some undesirable factors such as interface roughness, well width fluctuation, and random alloy disorder are hard to avoid under non-optimal growth condition. For example, the QW interface defects can trap carriers and influence their transport and recombination processes. This phenomenon, which is most apparent in cryogenic temperatures, can severely degrade the device performance.[6–10]

The optical properties of GaInAsSb/AlInAsSb QWs have been studied by several groups. Rainò *et al.*[9] studied the QWs using temperature dependent PL and obtained an energy level value of 8 meV, which they attributed to the binding energy of excitons bound to the localized defect states. The observed PL intensity degradation as temperature rises (PL quenching) at low temperatures was then attributed to the delocalization of carriers from the defect states. Similar results were also observed by Shen *et al.*[8] They compared the temperature dependence of the emission and absorption spectra and found a relatively large stokes shift of ~8 meV at 4 K and nearly none (<2 meV) at high temperatures. All these results indicate the existence of localized states in the QWs, and they play an important role in the optical property of these QWs.

Advance growth techniques for improving the QW/barrier interfaces have been widely studied.[11–15] Interface treatments included strain control in the layers, growth interruption and shutter sequencing at the interfaces between the wells and barriers. The significant improvement in material quality,[11–13] lasing threshold current density,[14] as well as characteristic temperature[15] for GaInAsSb QW lasers has been demonstrated.

In this work, the GaInAsSb/AlGaAsSb double QWs were grown on (001) GaSb substrates by MBE with our recently developed novel growth technique. The optical properties of this quaternary material system were studied in detail using power and temperature dependent PL measurements. We found that, with our growth technique, the defect induced exciton localization problem is nearly absent in our samples. The PL quenching at low temperatures no longer exists. Both the PL intensity and the line width were improved significantly.

II. SAMPLES AND EXPERIMENTS

The samples investigated were grown on (001) n-type GaSb substrates by a Veeco GEN II MBE system. As_2 and Sb_2, the group-V sources, were supplied by the valved cracker cells. After desorption of native oxide, a 200 nm thick GaSb was grown first to smooth the surface. We then grew the double QWs, which consisted of two 10 nm thick compressively strained $Ga_{0.65}In_{0.35}As_{0.13}Sb_{0.87}$ QWs, which were separated by a 20 nm thick slightly tensile strained $Al_{0.3}Ga_{0.7}As_ySb_{1-y}$ barrier layer. The two QWs were sandwiched between two 250 nm thick $Al_{0.3}Ga_{0.7}As_{0.03}Sb_{0.97}$ layers. Finally, a 20 nm thick GaSb cap layer was grown on

[a]E-mail: chlin.ee97g@g2.nctu.edu.tw

 © 2014 AIP Publishing LLC

[This article is copyrighted as indicated in the article. Reuse of AIP content is subject to the terms at: http://scitation.aip.org/termsconditions. Downloaded to] IP: 140.113.38.11 On: Tue, 21 Jul 2015 10:10:05

the top surface. The growth rates for barrier and QW were set to 0.72 μm/h and 0.77 μm/h, respectively. The growth temperature was measured by the infrared pyrometer, calibrated to the GaSb oxide desorption temperature of 510 °C under Sb_2 environment. The growth temperature for the GaSb and bottom AlGaAsSb layers was 500 °C. The temperature was lowered to 450 °C for the QWs. After that, the temperature was raised to 480 °C for the remaining layers. The relatively lower growth temperature for the top AlGaAsSb layer was to avoid the atomic inter-diffusion between the QWs and the barrier layers.

In order to improve the QW quality, we used a special growth and shutter control sequence, which is shown in Fig. 1. In MBE growth, a growth interruption procedure is commonly used at the QW/barrier interfaces[11,12] to obtain an abrupt layer transition. However, because the Sb aggregation and the exchange interaction between Sb_2 and As_2[16] may occur simultaneously during growth, disorder formation can easily happen. This material degradation has been confirmed by the high resolution x-ray diffraction (HRXRD) analysis reported by Li *et al.*[13] In our method, we performed the growth interruption earlier when the growth temperature was lowered. During this period of time, Sb_2 flux was kept as low as possible. We then did a few seconds Sb_2 and As_2 soak (the arrow head in Fig. 1) prior to the active region growth. We found that this procedure enhanced the QW optical properties significantly. When growth interruption was finished, we first grew a 10 nm barrier layer, which was following immediately by the QW growth without any pause.

To examine the material compositions and crystalline quality, we performed HRXRD measurement for our samples. For optical property analysis, PL measurements with the conventional lock-in method were carried out over the temperature range of 15 K to 300 K. An Ar-ion laser operated at 514.5 nm or a He-Ne laser at 632.8 nm was used as the excitation source; the luminescence was analyzed by a 0.55 m spectrometer and detected by a thermoelectrically cooled InGaAsSb photodetector.

III. DISCUSSIONS

The ω-2θ HRXRD spectrum in the (004) crystal plane of our sample together with the simulated result are showed in Fig. 2. The spectrum reveals well separated satellite peaks of

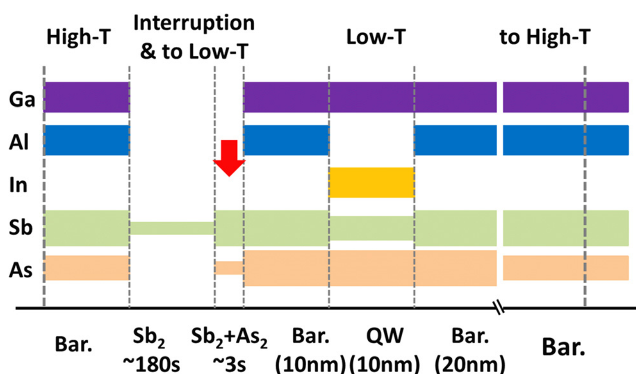

FIG. 1. The shutter control sequence during the growth of our sample. The thickness of the strips for group-V elements also indicates the beam flux.

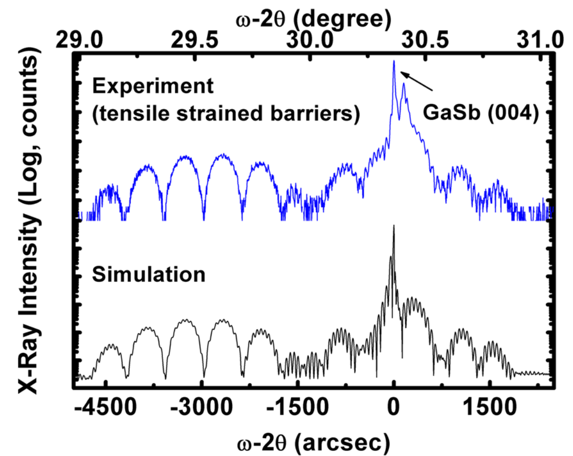

FIG. 2. Measured (004) HRXRD spectrum (top) of our sample (sample A) and the simulated spectrum (bottom).

the double QWs structure and clearly resolved Pendellösung fringes on both sides of the GaSb main peak, which indicates the good structural quality. Moreover, an interference modulation pattern around the GaSb peak, which is attributed to the slightly tensile strained $Al_{0.3}Ga_{0.7}As_ySb_{1-y}$ ($y \sim 0.07$) barriers neighboring to GaInAsSb QWs, is observed. As shown in Fig. 1, a constant As_2 flux was used throughout the growth of the active region. The slight tensile strain in the barriers due to the relative higher As incorporation served to compensate the compressive strain in the QWs. The simulated XRD spectrum based on the growth parameters is in good agreement with the measured result.

As we mentioned earlier, a few seconds of $Sb_2 + As_2$ soak prior to the active region growth can greatly enhance the QW optical properties. For comparison, we have grown two additional samples, besides the one mentioned above, with different growth conditions. Sample A is our standard sample with the growth procedure described above and in Fig. 1. Sample B was grown without the step of the $Sb_2 + As_2$ soak, and sample C had the $Sb_2 + As_2$ soak but used lattice matched barriers. The growth parameters are summarized in Table I. Fig. 3 shows the PL spectra of these three samples at temperatures of 15 K and 300 K. All samples exhibit similar emission wavelength around 2.2 μm at room temperature. Comparing these three spectra, we can see clearly, the PL intensities of the samples with $Sb_2 + As_2$ soak (A and C) are about one order of magnitude higher than that of the sample without $Sb_2 + As_2$ soak. The full width at half maximum (FWHM) is also narrower for the samples with $Sb_2 + As_2$ soak (see in Table I). It is known, the Sb_2 soak during the interruption step may lead to unintentional Sb aggregation at the interface. But the presence of As_2 during the soaking period would consume the undesirable Sb aggregation by the efficient exchange interaction between Sb and As. This effectively clear up the interface without accumulated Sb. However, we have to be very careful about the soaking time because excessive soaking can cause too much exchange interaction and that can degrade the interface too. Additionally, comparing sample A with sample C, we can see that with additional tensile strain in the barrier layer, the PL intensity can stay strong even at room temperature. The

[This article is copyrighted as indicated in the article. Reuse of AIP content is subject to the terms at: http://scitation.aip.org/termsconditions. Downloaded to] IP: 140.113.38.11 On: Tue, 21 Jul 2015 10:10:05

TABLE I. Growth parameters of the three GaInAsSb double QWs as well as their emission wavelength and FWHM.

Sample	Soak prior to active region	AlGaAsSb barrier layer	Wavelength (μm) FWHM (meV) at 15 K	Wavelength (μm) FWHM (meV) at 300 K
A	180s Sb_2 + 3s Sb_2 and As_2	Tensile strained	1.964 (6.1)	2.202 (25.2)
B	180s Sb_2	Tensile strained	1.993 (10.6)	2.226 (27.2)
C	180s Sb_2 + 3s Sb_2 and As_2	Lattice matched	1.942 (7.6)	2.162 (23.6)

reduction of PL quenching at high temperatures is probably caused by the increase of the valence band offset in the structure due to more As content in the tensile strained barrier layers.

Fig. 4(a) shows the temperature dependence of the PL spectrum of sample A under low excitation level (5 W/cm^2). The peak emission energy versus temperature is plotted in Fig. 4(b). Using the Varshni relationship and the fitted parameters in the high temperature region, we calculated the bandgap energy as a function of temperature.[17] The calculated curve is also shown in Fig. 4(b). Nearly, a perfect fit was obtained. Contrast to similar material systems reported before,[8,9] a very small deviation (from the ideal Varshni relationship) of 1.6 meV at 15 K was obtained. It indicates the excitonic localization effect caused by imperfect QW structures is very minimal in our samples. To have a better examination of the material quality, we have also studied the PL line shape. It is well known that the spectrum in a high quality QW exhibits a Lorentzian distribution function due to finite lifetime of the carrier recombination.[18] However, the imperfection in the QWs would lead to the spectral inhomogeneous broadening, especially at cryogenic temperatures. The line shape of the low temperature PL was fitted by the following expression:

$$I_{PL}(h\upsilon) \propto erfc\left(\frac{E_g - h\upsilon}{\sqrt{2}\cdot\sigma}\right)\cdot\exp\left(-\frac{h\upsilon - E_g}{k_B T}\right), \quad (1)$$

where E_g is the bandgap energy, $h\nu$ is the photo energy, and σ is the fitting parameter for the inhomogeneous broadening.

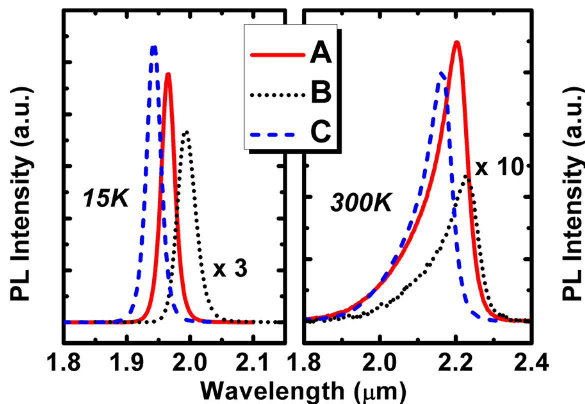

FIG. 3. The PL spectra of sample A (red solid line), sample B (black dot line), and sample C (blue dash line) at 15 K and 300 K. Growth parameters of samples A–C are listed in Table I.

The fitted curve along with the measured spectrum at 15 K is shown in the inset of Fig. 4(a). The fitted value of σ was only 2.4 meV. Such narrow line width indicates that the QWs had excellent material quality, very smooth well/barrier interfaces and were free of localized exciton states.

As the temperature rises, the emission intensity drops. In our sample, the integrated intensity drops less than seven times from 15 K to 300 K. This indicates that the QWs are very efficient emitters even at room temperature. We have fitted the integrated emission intensity as a function of excitation power using the well known equation,[19] $I_{PL} = \eta I_{ex}^{\alpha}$, where η is the PL efficiency and α is in the range of 1–2 depending on the radiative recombination mechanisms. Fig. 5 shows the PL integrated intensity as a function of

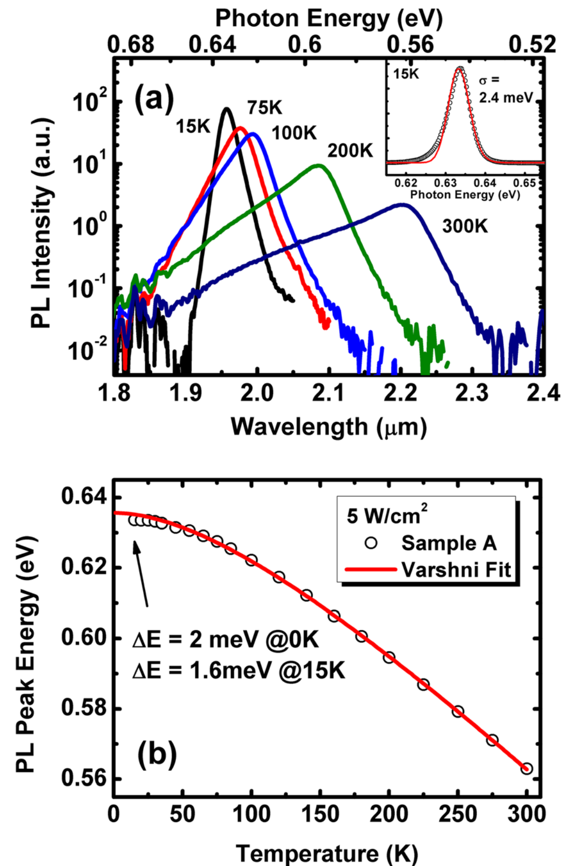

FIG. 4. (a) The PL spectra of sample A at various temperatures with low excitation power density. Inset shows the PL band width analysis at 15 K. (b) The PL peak energy as a function of temperature. The solid curve is based on Varshni relation which is obtained by the best fitting with experimental data in the high temperature region.

[This article is copyrighted as indicated in the article. Reuse of AIP content is subject to the terms at: http://scitation.aip.org/termsconditions. Downloaded to] IP: 140.113.38.11 On: Tue, 21 Jul 2015 10:10:05

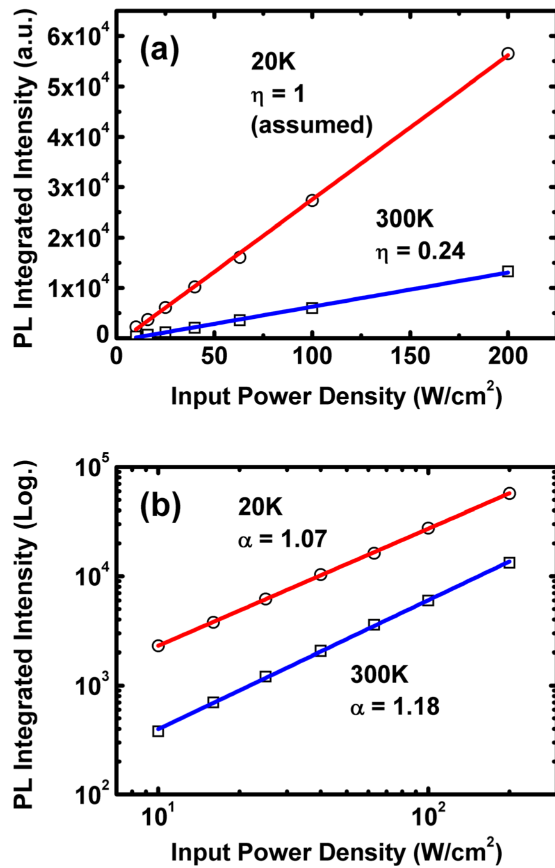

FIG. 5. PL integrated intensity in sample A as a function of excitation power density in linear scale (a) and log-log scale (b) at 20 K (circles) and 300 K (squares).

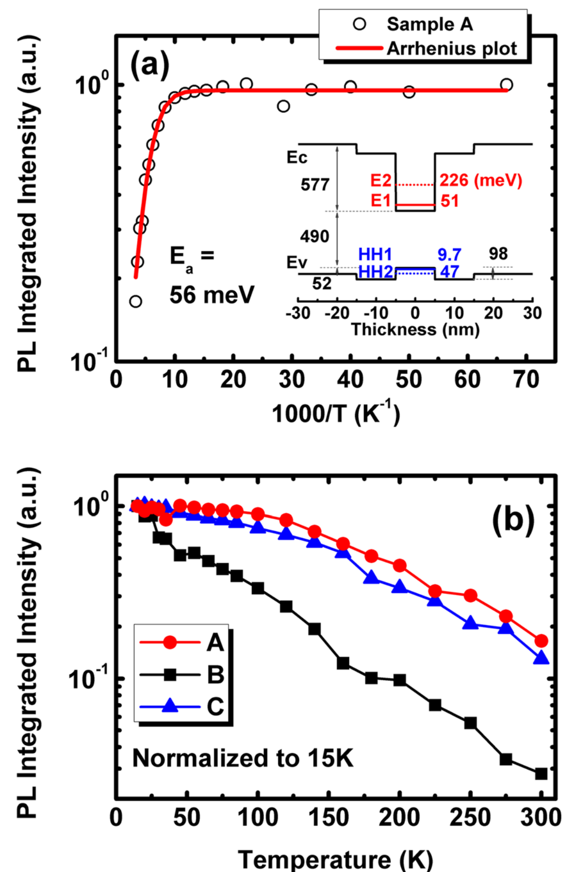

FIG. 6. (a) The PL integrated intensity of sample A as a function of inverse temperature. The solid line is the fitted curve using a single thermal activated process. Inset shows the calculated band lineups of the QW. (b) Temperature dependence of PL integrated intensity of sample A (red circles), B (black squares), and C (blue triangles).

excitation power density at 20 K and 300 K along with the fitted curve. From the linear plot shown in Fig. 5(a), we can see that the α value is very close to one. If we assume that η equals one at 20 K, the calculated η at room temperature is 0.24. It shows again that the PL efficiency remains high even at high temperatures. Examining carefully the log-log plot shown in Fig. 5(b), we obtain α values of 1.07 and 1.18 at 20 K and 300 K, respectively. It is known that $\alpha = 1$ indicates excitonic recombination while $\alpha = 2$ indicates free electron-hole pair recombination. The fact that the α values are close to one in our samples both at low temperatures and room temperature shows the recombination mechanism in our QWs is dominated by the more efficient exciton recombination. In the measurement range, that we have used (up to 300 K and 200 W/cm^2), the fact that $\alpha \sim 1$ also indicates that Auger recombination is probably not important because it would result in a sublinear behavior in the integrated PL intensity versus excitation power relationship.

To gain a further understanding on the PL quenching mechanism at high temperatures, we plot the PL integrated intensity versus inverse temperature of sample A in Fig. 6(a). The intensity stays nearly constant at low temperatures up until 75 K. It then drops down as the temperature goes further up. A single thermal activated process is observed with an activation energy of 56 meV. This is quite different from previous reports on similar material systems, where two different activation processes were observed.[8,9] One was the delocalization of the bound excitons from the defect states in the QWs (which has an activation energy around 10 meV), and the other was the over the barrier excitation after the carriers were delocalized. In other words, in those samples the radiative radiation at low temperatures is dominated by the recombination of bounded excitons which are trapped in the QW defect states with a binding energy $\sim$10 meV. As the temperature is increased, the excitons are ionized and the PL intensity drops because the carriers escape from the QWs and that has a higher activation energy. But in our sample, the 10 meV delocalization process was absent. It again shows our sample is free from those defect states that cause exciton localization and that is why the integrated intensity of our sample could stay constant at low temperatures. The observed activation energy of 56 meV for our sample at high temperatures is caused by the escape of holes from the QWs. Based on our calculation, this energy corresponds to the energy difference between the second heavy hole sub-band in the QW and the valence band edge in the barriers.[20–22] So the major quenching mechanism in our sample is attributed to bounded holes thermalizing from QWs to surrounding barriers.

We have also compared the PL quenching behaviors between three samples described earlier. Samples A and C

[This article is copyrighted as indicated in the article. Reuse of AIP content is subject to the terms at: http://scitation.aip.org/termsconditions. Downloaded to] IP: 140.113.38.11 On: Tue, 21 Jul 2015 10:10:05

had the short $Sb_2 + As_2$ soaking step at the interfaces, while sample B did not. The integrated intensity versus temperature plot is shown in Fig. 6(b). A very clear difference in the PL quenching behavior is observed between samples A–C. The PL intensity of sample B starts to drop quickly even at low temperatures, but those of samples A and C do not. So, the $Sb_2 + As_2$ soaking step plays a crucial role in the PL intensity quenching. This step effectively removes the defect states at the QW/barrier interfaces and reduces the PL quenching. We also observe an improvement in the PL integrated intensity in the strain compensated sample (A) in all temperatures.

Fig. 7(a) shows the PL spectra of sample A from 15 K to 300 K in linear scale and in log scale (inset). The FWHM of the spectrum increases as temperature rises as shown in Fig. 7(b). At low temperature limit, the inhomogeneous broadening gives a limiting value around 5 meV, which is smaller than what were reported previously in similar material systems. The mechanisms for the line width broadening of PL spectrum have been widely studied.[23–26] Theoretically, there are several mechanisms that can contribute to the line width broadening. The temperature dependence of these mechanisms can be described as

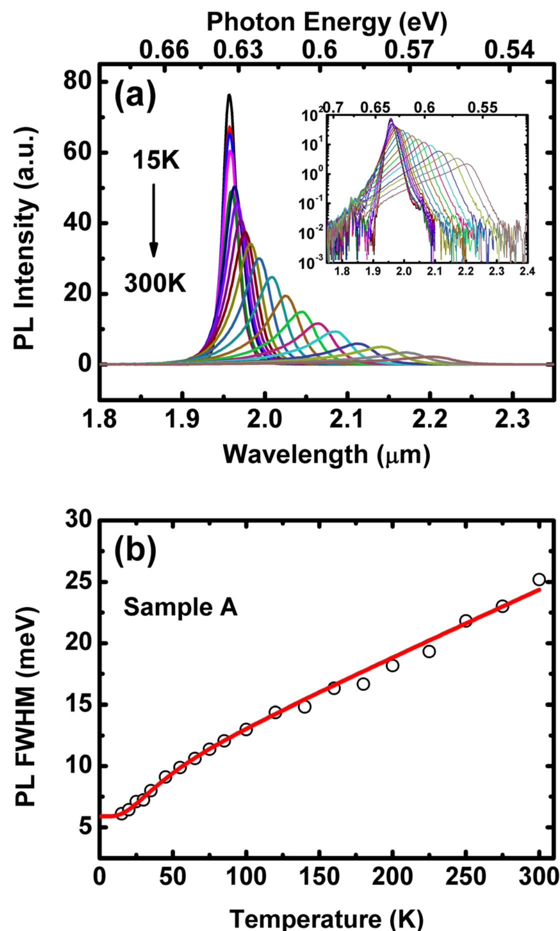

FIG. 7. (a) The PL spectra of sample A from 15 K to 300 K in linear scale and in log scale (inset). (b) Temperature dependence of PL FWHM of sample A along with the fitted curve which contains homogeneous- and inhomogeneous broadening.

$$
\begin{aligned}
\Gamma(T) &= \Gamma(0) + \Gamma_a(T) + \Gamma_{LO}(T) + \Gamma_{im}(T),\\
\Gamma_a(T) &= \gamma_a T,\\
\Gamma_{LO}(T) &= \frac{\Gamma_{LO}}{\exp(\hbar\omega_{LO}/k_B T) - 1},\\
\Gamma_{im}(T) &= \Gamma_{im}\exp(-E_{im}/k_B T),
\end{aligned}
\tag{2}
$$

where $\Gamma_{LO}(T)$ is due to the LO phonon scattering, $\Gamma_a(T)$ is due to the acoustic phonon scattering, and $\Gamma_{im}(T)$ is the contribution from the ionized impurity scattering. The inhomogeneous broadening due to structural imperfection and other impurities gives the non-zero line width, $\Gamma(0)$ at $T = 0$ K. In Fig. 7(b), we also show the fitted curve using the expression shown above. The LO phonon energy $\hbar\omega_{LO}$ was assumed to be 29 meV, which was calculated by linear interpolation using the values of the constituent binary compounds.[8] Only the ionized impurity scattering and the optical scattering terms were considered in the fitting, and the curve fits the experimental result reasonably well. The fitting parameters show $\Gamma(0) = 5.9$ meV, $E_{im} = 5.3$ meV, $\Gamma_{im} = 12$ meV, and $\Gamma_{LO} = 18$ meV.

IV. CONCLUSIONS

In summary, we have developed a method for the growth of high quality GaInAsSb/AlGaAsSb QWs. Utilizing the nature of the anion (As and Sb) exchange, we were able to control the well/barrier interfaces using a proper shutter control sequence. The resulting QWs had excellent optical quality and were free from undesired localized trap states, which may otherwise severely affect the exciton recombination. Strong and highly efficient exciton emissions up to room temperature with a wavelength of 2.2 μm were observed. The temperature and power dependent PL measurements were used to characterize the QW properties in detail. The QWs exhibit a bulk-like temperature dependence of the bandgap energy (from PL emission peak). The integrated PL intensity remains nearly constant in the low temperature region. These all indicate that the excitons are not influenced by localized states caused by interface roughness and other material defects. The PL quenching mechanism at high temperatures was found to be caused by the escape of holes from the QW heavy-hole subband to the barriers. The spectral line width of the PL emission has a very small low temperature inhomogeneous broadening limit of only ∼5 meV, indicating excellent QW uniformity and interface smoothness.

ACKNOWLEDGMENTS

This work was supported by the Ministry of Science and Technology of Taiwan under Contract No. MOST 103-2221-E-009-005 and the Aiming for the Top University Program of the National Chiao Tung University and Ministry of Education of Taiwan. The authors would like to thank the equipment support from Center for Nano Science and Technology of National Chiao Tung University.

[1]K. Kashani-Shirazi, K. Vizbaras, A. Bachmann, S. Arafin, and M. C. Amann, IEEE Photonics Technol. Lett. **21**, 1106 (2009).

[This article is copyrighted as indicated in the article. Reuse of AIP content is subject to the terms at: http://scitation.aip.org/termsconditions. Downloaded to] IP: 140.113.38.11 On: Tue, 21 Jul 2015 10:10:05

[2]L. Shterengas, G. Belenky, M. V. Kisin, and D. Donetsky, Appl. Phys. Lett. **90**, 011119 (2007).
[3]R. Liang, J. Chen, G. Kipshidze, D. Westerfeld, L. Shterengas, and G. Belenky, IEEE Photonics Technol. Lett. **23**, 603 (2011).
[4]M. Grau, C. Lin, O. Dier, C. Lauer, and M. C. Amann, Appl. Phys. Lett. **87**, 241104 (2005).
[5]G. Belenky, L. Shterengas, G. Kipshidze, and T. Hosoda, IEEE J. Sel. Top. Quantum Electron. **17**, 1426 (2011).
[6]T. Takagahara, Phys. Rev. B **31**, 6552 (1985).
[7]D. S. Citrin, Phys. Rev. B **47**, 3832 (1993).
[8]W. Z. Shen, S. C. Shen, W. G. Tang, Y. Zhao, and A. Z. Li, J. Appl. Phys. **78**, 5696 (1995).
[9]G. Rainò, A. Salhi, V. Tasco, R. Intartaglia, R. Cingolani, Y. Rouillard, E. Tournié, and M. D. Giorgi, Appl. Phys. Lett. **92**, 101931 (2008).
[10]J. Thoma, B. Liang, L. Lewis, S. P. Hegarty, G. Huyet, and D. L. Huffaker, Appl. Phys. Lett. **102**, 113101 (2013).
[11]G. W. Turner, H. K. Choi, D. R. Calawa, J. V. Pantano, and J. W. Chludzinski, J. Vac. Sci. Technol., B **12**, 1266 (1994).
[12]E. Selvig, G. Myrvågnes, R. Bugge, R. Haakenaasen, and B. O. Fimland, Phys. Scr. **T126**, 110 (2006).
[13]W. Li, H. Shao, D. Moscicka, T. Unuvar, and W. I. Wang, IEEE Photonics Technol. Lett. **17**, 2274 (2005).
[14]K. Vizbaras, A. Bachmann, S. Arafin, K. Saller, S. Sprengel, G. Boehm, R. Meyer, and M. C. Amann, J. Cryst. Growth **323**, 446 (2011).
[15]W. Li, J. B. Héroux, H. Shao, and W. I. Wang, IEEE Photonics Technol. Lett. **17**, 531 (2005).
[16]M. Losurdo, P. Capezzuto, G. Bruno, A. S. Brown, T. Brown, and G. May, J. Appl. Phys. **100**, 013531 (2006).
[17]Y. P. Varshni, Physica (Utrecht) **34**, 149 (1967). The parameters, α and β, in the Varshni equation are 3.95×10^{-4} eV/K and 188 K, respectively, according to the experimental data obtained at high temperature region which are closed to the calculated values of bulk $Ga_{0.65}In_{0.35}As_{0.13}Sb_{0.87}$ by linearly interpolated method using the binary values (α_{cal} and β_{cal} are 3.91×10^{-4} eV/K and 152 K, respectively).
[18]J. Christen and D. Bimberg, Phys. Rev. B **42**, 7213 (1990).
[19]S. Jin, Y. Zheng, and A. Li, J. Appl. Phys. **82**, 3870 (1997).
[20]The band lineups calculation is performed by K·P method with parameters given in Ref. 21. The bandgaps of the quaternary materials used in the calculation were referred to Ref. 22.
[21]I. Vurgaftman, J. R. Meyer, and L. R. Ram-Mohan, J. Appl. Phys. **89**, 5815 (2001).
[22]G. P. Donati, R. Kaspi, and K. J. Malloy, J. Appl. Phys. **94**, 5814 (2003).
[23]S. Rudin, T. L. Reinecke, and B. Segall, Phys. Rev. B **42**, 11218 (1990).
[24]A. V. Gopal, R. Kumar, A. S. Vengurlekar, A. Bosacchi, S. Franchi, and L. N. Pfeiffer, J. Appl. Phys. **87**, 1858 (2000).
[25]J. Lee, E. S. Koteles, and M. O. Vassell, Phys. Rev. B **33**, 5512 (1986).
[26]H. Zhao and H. Kalt, Phys. Rev. B **69**, 233305 (2004).

[This article is copyrighted as indicated in the article. Reuse of AIP content is subject to the terms at: http://scitation.aip.org/termsconditions. Downloaded to] IP: 140.113.38.11 On: Tue, 21 Jul 2015 10:10:05